ELSEVIER

Contents lists available at ScienceDirect

# Science of the Total Environment

journal homepage: www.elsevier.com/locate/scitotenv





# Long-term trends in inorganic aerosol chemical composition and chemistry at an urban and rural site in the northeastern US

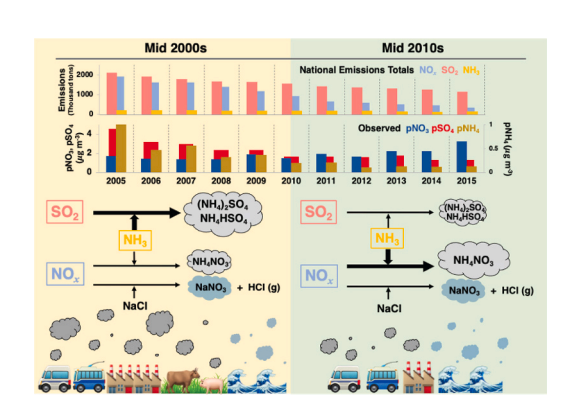
Heejeong Kim<sup>a,b</sup>, Wendell W. Walters<sup>a,b,\*</sup>, Lizzy Kysela<sup>c</sup>, Meredith G. Hastings<sup>a,b</sup>

- a Department of Earth. Environmental, and Planetary Sciences. Brown University, Providence, RI 02912, USA
- <sup>b</sup> Institute at Brown for Environment and Society, Brown University, Providence, RI 02912, USA
- <sup>c</sup> Center for Sustainability and the Global Environment, University of Wisconsin-Madison, Madison, WI 53726, USA

#### HIGHLIGHTS

- $\bullet$  Inorganic chemical compositions determined from a 2005–2015  $PM_{10}$  aerosol record in the Northeastern US.
- Significant reduction in SO<sub>2</sub> emissions led to reduction in particulate sulfate and ammonium.
- More localized ammonium aerosol formation is apparent in recent years.
- Despite significant  $NO_x$  reductions, aerosol nitrate increased due to decrease in atmospheric acidity.
- Aerosol nitrate is expected to continuously increase as atmospheric acidity decreases.

## G R A P H I C A L A B S T R A C T



# ARTICLE INFO

Editor: Jianmin Chen

Keywords: Aerosols PM<sub>10</sub> Nitrate Sulfate Ammonium

Clean Air Act

# ABSTRACT

Atmospheric nitrate and sulfate are major inorganic particulate matter components that impact human and ecosystem health and air quality. Over the last several decades, emissions of the precursor gases, nitrogen oxides  $(NO_x = NO + NO_2)$  and sulfur dioxide (SO<sub>2</sub>), have dramatically decreased in the US in response to federal regulations. However, the response in concentrations of particulate nitrate (pNO<sub>3</sub>) and sulfate (pSO<sub>4</sub>) have not followed predictions due to complex non-linear chemistry feedbacks that may differ amongst environments (i.e., urban vs. rural). In this study, we explored the long-term response of particle chemistry for urban and rural environments in southern New England, a region historically impacted by NOx and SO2 emissions. Particulate matter (PM<sub>10</sub>) samples collected via the same method from 2005 to 2015 at urban and rural locations in Rhode Island were analyzed for their major inorganic components, and air mass trajectories and statistical analysis were used to identify source regions over time. Our results indicated a significant urban-rural aerosol chemical composition gradient for sampling locations within 40 km. Over time, as anthropogenic influences have decreased, the relative contribution of marine and crustal sources has increased greatly, impacting fine and coarse particle chemistry in recent years. Total mass concentrations of chemical species, particularly anthropogenic pSO<sub>4</sub> and particulate ammonium (pNH<sub>4</sub>), have shown dramatic decreases over the ten years at both the urban and rural sites; however, pNO<sub>3</sub> concentration increased by 95 % and 57 % in the urban and rural sites, respectively, despite significant  $NO_x$  emission reductions. Our results demonstrate that changes in chemical

<sup>\*</sup> Corresponding author at: Department of Chemistry and Biochemistry, University of South Carolina, Columbia, SC 29208, USA. *E-mail address:* wendellw@mailbox.sc.edu (W.W. Walters).

mechanisms due to the decrease in  $SO_2$  emissions contributed to decreases in pNH<sub>4</sub>, along with enhanced pNO<sub>3</sub> concentration. Furthermore, the change in  $SO_2$  emissions has significantly impacted the atmospheric lifetime and transport distance of pNH<sub>4</sub>, favoring more localized contributions in recent years.

#### 1. Introduction

Atmospheric particulate matter (PM) is a critical atmospheric pollutant originating from various natural (e.g., sea salt particles and wind-blown dust) and anthropogenic activities (e.g., industrial activities, vehicle, and combustion processes) (O'Dowd et al., 1997; Manisalidis et al., 2020; Lenschow et al., 2001; Harrison et al., 1997). PM<sub>10</sub>, a particle with diameters smaller than  $10 \mu m$ , has potential adverse air quality and climate change impacts as well as human and ecosystem health (Seinfeld, 1998; Fuzzi et al., 2015; Camargo and Alonso, 2006; Schlesinger, 2007). For example, high concentrations of PM<sub>10</sub> are directly associated with the acidity of clouds, visibility degradation, and solar radiation transfer, which can lead to poor air quality and affect the atmosphere's radiative properties (Pye et al., 2020; Hyslop, 2009; Andreae et al., 2005). In terms of health effects, epidemiological studies have shown that the level of PM<sub>10</sub> has a direct connection with respiratory illnesses such as asthma, pulmonary damage, or mortality rate (Donaldson et al., 2000; Wilson and Suh, 1997; Scanlon et al., 2000; Berico et al., 1997; Dominici et al., 2002; Orellano et al., 2020). Further, inorganic components in PM<sub>10</sub>, such as particulate sulfate (pSO<sub>4</sub>), particulate nitrate (pNO<sub>3</sub>), and particulate ammonium (pNH<sub>4</sub>), negatively impact sensitive ecosystems causing eutrophication, soil acidification, and forest degradation (Van Breemen and Van Dijk, 1988; Bobbink et al., 1998).

Over the past several decades, emissions of the precursor gases, sulfur dioxide (SO<sub>2</sub>), and nitrogen oxides (NO<sub>x</sub> = NO + NO<sub>2</sub>), deriving from industrialization and urbanization, have caused severe PM<sub>10</sub> pollution in the US. The Clean Air Act Amendments (CAAA) of 1990 were implemented in the US to reduce major environmental threats such as acid rain, urban air pollution, and toxic air emissions. In response to the CAAA in the US, SO<sub>2</sub> and NO<sub>x</sub> emissions were successfully controlled with a total decrease of 73 % and 43 %, respectively, between 2005 and 2015, leading to a decrease in average PM<sub>10</sub> concentrations at the national level (US EPA, 2017; NEI, 2017; Shah et al., 2018; Jaeglé et al., 2018). The US Environmental Protection Agency (EPA) has continuously monitored PM<sub>10</sub> concentrations throughout the country to improve air quality and set the national air quality standards for PM<sub>10</sub> (24-hour standards with one-expected exceedance forms and levels of 150 μg m<sup>-3</sup>, US EPA, 2017). Long-term monitoring of speciated air pollutants has been conducted at several national monitoring networks in the US, including the Clean Air Status and Trends Network (CAST-NET), the Chemical Speciation Network (CSN), the Interagency Monitoring of Protected Visual Environments (IMPROVE), the National Atmospheric Deposition Program (NADP), and the Ammonia Monitoring Network (AMoN). However, these networks utilize different techniques for sample collection depending on the network goals, such that it can be challenging to integrate data and compare measurements across the various monitoring networks. For example, the CASTNET program monitors total suspended particles (TSP) collected on a Teflon filter, primarily in rural locations, while the CSN program collects fine PM (PM<sub>2.5</sub>) using Nylon filters in urban locations. The different types of filters have different collection biases and artifacts, making it difficult to make quantitative comparisons across networks and landscapes (i.e., urban versus rural). Compared to several national monitoring networks, our PM<sub>10</sub> records are simultaneously sampled using the same methodology between rural and urban locations which motivated this research.

The northeastern US has been an important region to monitor as its high population density and transport patterns have affected the degradation of air quality (Sickles II and Shadwick, 2015). Reductions of  $SO_2$  and  $NO_x$  in the northeastern US have been even more impressive,

with decreases of 46 % and 82 %, respectively, since 2005 (NEI, 2017). However, the responses in pSO<sub>4</sub> and pNO<sub>3</sub> concentrations have not been as strong as the precursor emission reduction due to the complex nonlinear chemistry feedback that may differ for varying environments (i. e., urban versus rural and summer versus winter). For example, atmospheric chemistry model (GEOS-Chem) simulation results showed that as SO<sub>2</sub> and NO<sub>x</sub> emissions decrease, aerosol pH and oxidation efficiency increase, leading to more effective secondary aerosol formation, especially for pNO<sub>3</sub> (Shah et al., 2018; Guo et al., 2016; Holt et al., 2015). Consequently, pNO<sub>3</sub> concentrations are expected to increase in the northeastern US as SO<sub>2</sub> emissions continuously decrease. A comprehensive understanding of aerosol chemical composition changes is clearly needed to design the emission reduction policy that can also target future particulate matter reductions.

This study aims to understand the connection between precursor emissions changes and spatiotemporal variabilities of inorganic species in PM<sub>10</sub> utilizing aerosol samples that were simultaneously collected using the same protocol at an urban and rural site in the northeastern US between 2005 and 2015. In the northeastern US, particle pollution levels are exacerbated by the combination of high population density, heavilydeveloped industrial and transportation sectors, and natural influences (e.g., marine and crustal), making it difficult to target effective strategies for mitigating air quality. This study aims to explore key uncertainties in the production mechanisms of major anthropogenic inorganic species (e.g., pNO<sub>3</sub>, pSO<sub>4</sub>, and pNH<sub>4</sub>; note that all components of particulate matter are referred to as pX, where X represents nitrate, sulfate, ammonium, sodium, etc.) in response to emission regulation implementation with an emphasis on seasonal and spatial patterns. By comparing urban and rural areas, it is possible to better understand the impacts of different emission sources and their changes on the chemistry of inorganic species in PM<sub>10</sub>. Detailing the changes in oxidation chemistry and chemical feedbacks associated with the production and deposition of inorganic species can have important implications for testing chemical model mechanisms, better predicting air quality improvements, and informing future policy recommendations.

### 2. Methods

# 2.1. Sampling and chemical analysis

PM<sub>10</sub> samples were collected at two different environmental sites in the state of Rhode Island, United States, including downtown Providence (41.82 $^{\circ}$  N,  $-71.41^{\circ}$  W) and West Greenwich (41.61 $^{\circ}$  N,  $-71.72^{\circ}$ W), representing an urban and rural environment, respectively (Fig. 1). Providence has a population of 191,000 and is an urban-mixed-use region that includes commercial buildings, residential buildings, highways, and industry (Fig. 1b). West Greenwich has a population of 6500, and the measurement site is in a meadow surrounded by trees. Forest and recreation fields are the major land use type in this area (Fig. 1b). Sample collections were conducted by the Rhode Island Department of Environmental Management (RI-DEM) and Rhode Island Department of Health (RI-DOH) using a high-volume sampler with a flow rate of 1.13  $\mathrm{m}^3\,\mathrm{min}^{-1}$ . Filter samples were collected on a quartz-fiber filter every six days for 24 h, following EPA protocols (USEPA-Method IO-2.1, 1999) from 2005 to 2015. Samples were measured for total mass concentration of PM<sub>10</sub> and stored at room temperature until transferred to Brown University in the summer of 2019.

Filter samples were extracted and analyzed for ion concentrations at Brown University. Briefly, filter cuts were taken and transferred to triple DI-rinsed Nalgene bottles and extracted in 100 mL of ultra-high purity water (MQ  $>18.2~\text{M}\Omega).$  Bottles were placed on a mechanical shaker table overnight. Filters were removed from the bottles, and then the extracted solution was filtered with a 0.2  $\mu m$  Nylon Filter and placed in a freezer until subsequent analysis. A subset of filters was extracted a second time with a separate volume of 100 mL. The second extraction was found to have ion concentrations always below detection limits, such that we assume our extraction technique fully characterizes the ion concentrations. The entire 2005–2015 record was extracted for the Providence location. A subset of samples was extracted for the endpoints of the West Greenwich record, including 2005–2006 and 2014–2015.

Major inorganic ion concentrations (i.e., sodium (Na<sup>+</sup>), potassium (K<sup>+</sup>), calcium (Ca<sup>2+</sup>), ammonium (NH<sub>4</sub><sup>+</sup>), magnesium (Mg<sup>2+</sup>), fluoride (F<sup>-</sup>), chloride (Cl<sup>-</sup>), nitrate (NO<sub>3</sub><sup>-</sup>), and sulfate (SO<sub>4</sub><sup>2-</sup>)) were analyzed using ion chromatography (Dionex Integrion HPIC) employing suppressed conductivity detection. Anions were determined using a Dionex AS19-4  $\mu m$  guard column (4  $\times$  50 mm) and analytical column (4  $\times$  250 mm) with 20 mM KOH as eluent and a flow rate of 1 mL min<sup>-1</sup>. Cations were analyzed using a Dionex CS-16 guard column (5 × 50 mm) analytical column (5  $\times$  250 mm). Eluent of 30 mM methane sulfonic acid (MSA) was used to detect cations with a pump flow rate of 1 mL min $^{-1}$ . Working standards of two different concentrations were analyzed every six samples for quality control. The limit of detection (LOD) for cations was 5.3 μM, 3.2 μM, 5.2 μM, 4.8 μM, and 4.7 μM for Na<sup>+</sup>, NH<sub>4</sub><sup>+</sup>, K<sup>+</sup>,  $Mg^{2+}$ , and  $Ca^{2+}$ , respectively and the LOD for anions was 0.6  $\mu$ M, 1.7  $\mu$ M, 1.2  $\mu$ M, and 4.0  $\mu$ M for F<sup>-</sup>, Cl<sup>-</sup>, NO<sub>3</sub>, and SO<sub>4</sub><sup>2-</sup>, respectively. The average relative standard deviations (RSD) of replicate quality control standards were <3.4 % for all analyzed ions. For high NH<sub>4</sub><sup>+</sup> concentrations, over 250 µM, samples were rerun using standard colorimetric methods (i.e., US EPA Method 353.2) on an automated discrete UV-Vis Analyzer (SmartChem Westco Scientific Instruments, Inc.).

## 2.2. Sea salt and crustal calculation

The contributions of sea salt, crustal dust, and anthropogenic emissions to the PM<sub>10</sub> inorganic concentrations were calculated following

previous studies (Huang et al., 2008; Meng et al., 2019; Nah et al., 2021). (Note again that all components of particulate matter are referred to as pX, where X represents nitrate, sulfate, ammonium, sodium, etc.). The concentration unit was converted from the concentration in solution  $(\mu M)$  to the concentration in the air  $(\mu g m^{-3})$ , based on the extraction volume and the amount of sampled air, which typically corresponded to 1700 m<sup>3</sup> for each filter. The measured pNO<sub>3</sub>, pNH<sub>4</sub>, and pF were assumed to be solely derived from anthropogenic sources in this study. Other ions such as pCl, pSO<sub>4</sub>, and soluble nonvolatile cations (NVCs, such as pNa, pK, pCa, and pMg) are expected to derive from marine or crustal origins (Sun et al., 2006; Jayarathne et al., 2014; Meng et al., 2019); thus, their contributions were calculated separately. For example, pCl in PM<sub>10</sub> is generally considered to originate from sea salt with pNa or anthropogenic sources. The ratio of pCl and pNa originating from sea salt typically has a value of 1.8 (McInnes et al., 1994): if the ratio is greater, it is assumed that additional anthropogenic sources are contributing pCl (e.g., combustion processes). However, in our study, the observed pCl/pNa ratios were much lower than 1.8, indicating strong pCl depletion in the study areas, such that pNa was considered a better tracer of sea salt (see Section 4.1). The sea salt (SS) origin of pCa, pMg, pK, and pSO<sub>4</sub> can be estimated using volume-weighted concentration ( $\mu g m^{-3}$ ) as follows (Eqs. (1)–(4); Kennish, 2019; Huang et al., 2008; Nah et al., 2021):

$$[pCa]_{SS} = 0.037 \times pNa \tag{1}$$

$$[pMg]_{SS} = 0.012 \times pNa \tag{2}$$

$$[pK]_{SS} = 0.037 \times pNa \tag{3}$$

$$[pSO_4]_{SS} = 0.25 \times pNa \tag{4}$$

In addition to sea salt, pMg, pCa, pK, and pSO<sub>4</sub> were considered to have a crustal origin. The contribution of crustal sources to  $PM_{10}$  was quantified using non-sea salt (NSS) or crustal pMg as a reference. The crustal contribution of pCa, pK, and pSO<sub>4</sub> was calculated as follows (Eqs.

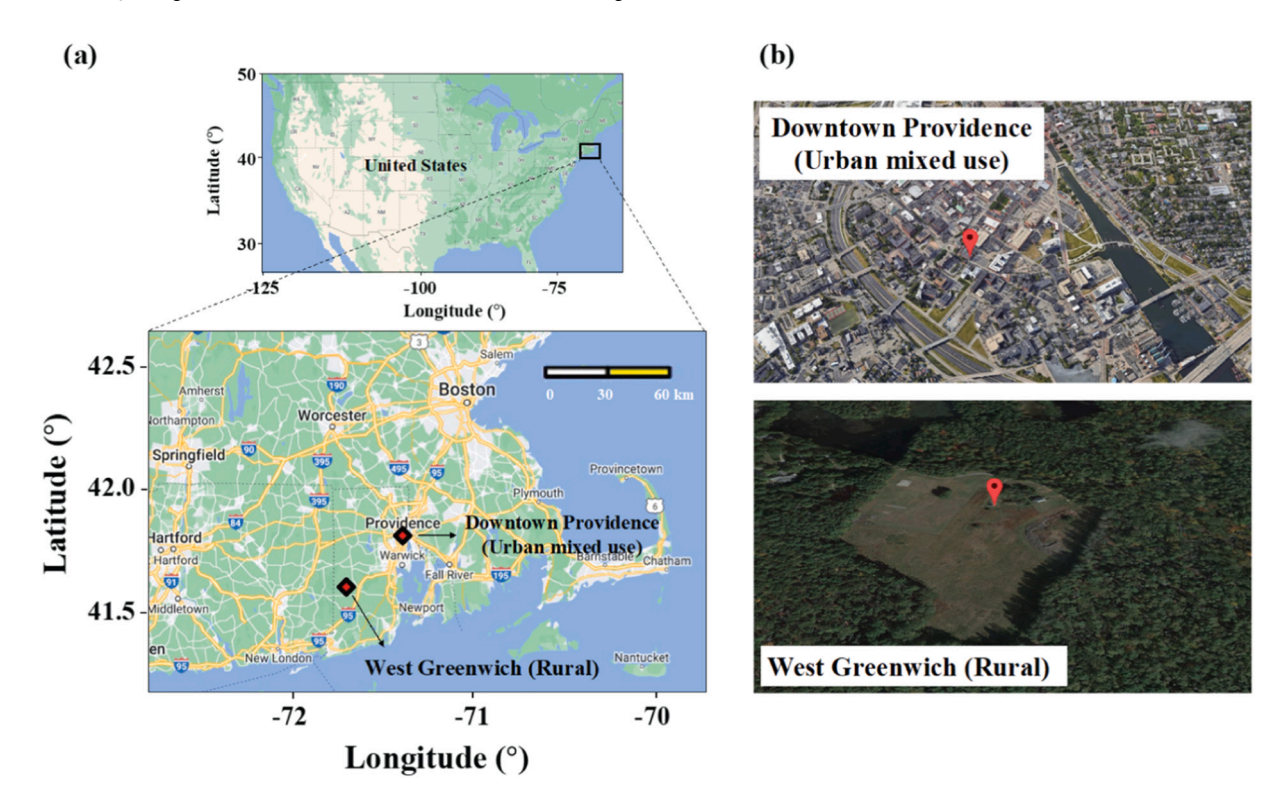


Fig. 1. Map of the (a) United States and Rhode Island and (b) two sampling sites in Rhode Island. Major cities (urban areas), transportation routes, and sampling sites are also indicated. The image was created using Google Earth (©2023 Google).

(5)-(7):

$$[pMg]_{NSS} = [pMg]_{crustal} = [pMg]_{total} - [pMg]_{SS}$$
(5)

$$[pCa]_{crustal} = [pMg]_{NSS} \times 1.87$$
 (6)

$$[pK]_{crustal} = [pMg]_{NSS} \times 0.48 \tag{7}$$

where 1.87 and 0.48 represent the equivalent ratio of pCa/pMg and pK/pMg in the crust, respectively (Huang et al., 2008). Mineral dust derived from calcium sulfate (CaSO<sub>4</sub>) contributes to the supply of pSO<sub>4</sub>; thus, [pSO<sub>4</sub>]<sub>crustal</sub> was calculated using the pCa/pSO<sub>4</sub> mass-ratio (Eq. (8); Delmas, 1981).

$$[pSO_4]_{crustal} = 0.47 \times [pCa]_{crustal}$$
(8)

The anthropogenic contributions of components with multiple origins, including pCa, pK, and pSO<sub>4</sub>, were calculated as the difference between the measured total and the amount of sea salt and crustal contribution (Eqs. (9)–(11); Meng et al., 2019).

$$[pSO4]anthropogenic = [pSO4]total - [pSO4]SS - [pSO4]crustal$$
(9)

$$[pCa]_{anthropogenic} = [pCa]_{total} - [pCa]_{SS} - [pCa]_{crustal}$$
(10)

$$[pK]_{anthropogenic} = [pK]_{total} - [pK]_{SS} - [pK]_{crustal}$$
(11)

If the calculated components of crustal and anthropogenic sources were negative, the values were substituted with 0  $\mu g$  m $^{-3}$ . These treatments of negative concentrations affected  $\sim\!0.4\,\%$  of the total data set for [pMg]\_crustal, leading to a 0.001  $\mu g$  m $^{-3}$  increase in the averaged concentration of [pMg]\_crustal. Further, for anthropogenic source calculations, the treatment of negative concentrations affected 2 %, 10 %, and 28 % of the total data set for [pSO\_4]\_anthropogenic, [pCa]\_anthropogenic, and [pK]\_anthropogenic, respectively. Though negative values account for a large portion of the anthropogenic sources data set, substitution to 0  $\mu g$  m $^{-3}$  leads to only 0.001  $\mu g$  m $^{-3}$ , 0.006  $\mu g$  m $^{-3}$ , and 0.007  $\mu g$  m $^{-3}$  increase in total averaged concentration of [pSO\_4]\_anthropogenic, [pCa]\_anthropogenic, and [pK]\_anthropogenic, respectively.

# 2.3. Back trajectory and PSCF analysis

Air-mass back trajectories were traced using the hybrid singleparticle Lagrangian integrated trajectory (HYSPLIT) model with the North American Regional Reanalysis (NARR) 12 km dataset (Stein et al., 2015). 72-Hour backward trajectories of air masses arriving at 1000 m above ground level were calculated every 6 h for the two sampling sites (Providence and West Greenwich, RI). Back trajectories were analyzed from 2005 to 2006, 2009 to 2010, and 2014 to 2015 for Providence and from 2005 to 2006 and 2014 to 2015 for West Greenwich. The trajectory data was collated with the main measured anthropogenic components, including pNO<sub>3</sub>, pSO<sub>4</sub>, and pNH<sub>4</sub> concentration data at a weekly resolution to compute the potential source contribution function (PSCF), which is a probability function indicating possible source locations (Ashbaugh et al., 1985; Zeng and Hopke, 1989; Wang et al., 2006). The PSCF analysis was calculated and plotted using the Trajstat software (Wang et al., 2009). The domain was 20-70°N and 40-110°W with horizontal resolutions of  $1^{\circ} \times 1^{\circ}$ . PSCF is defined as

$$PSCF_{ij} = \frac{m_{ij}}{n_{ij}} \tag{12}$$

where i is latitude, j is longitude,  $n_{ij}$  is the number of trajectories endpoints that fall in the grid cell, and  $m_{ij}$  is the number of trajectories endpoints above the criterion value of pollutants reaching the grid cell. To reduce the uncertainty in the cells with a small  $n_{ij}$  value, the PSCF values were multiplied by a weight function (i.e.,  $W_{ij}$ ) as follows:

Weighted PSCF (WPSCF) = 
$$W_{ij} \times PSCF$$
 (13)

 $W_{ii}$  is defined as below.

$$W_{ij} = \begin{cases} 1.00, 80 < n_{ij} \\ 0.70, 20 < n_{ij} \le 80 \\ 0.42, 10 < n_{ij} \le 20 \\ 0.05, n_{ij} \le 10 \end{cases}$$
 (14)

#### 2.4. Emissions inventory

The US EPA National Emissions Inventory (NEI) reports national emissions data by locations, sectors, and years. We used emission inventory data to investigate the trends in anthropogenic emissions of SO<sub>2</sub>, NO<sub>x</sub>, and ammonia (NH<sub>3</sub>) for our record from 2005 to 2015 (https://www.epa.gov/air-emissions-inventories/air-pollutant-emissions-trends-data, last access: April 11, 2023). Annual emissions inventory data of SO<sub>2</sub>, NO<sub>x</sub>, and NH<sub>3</sub> were obtained for the northeastern US, including Connecticut, New Jersey, New York, Pennsylvania, Massachusetts, New Hampshire, Rhode Island, and Vermont. This region was chosen because the back trajectory data indicated significant transport to the study sites from this area.

#### 3. Results

# 3.1. Inorganic chemical compositions of PM<sub>10</sub>

Prior chemical composition measurements are not available for the filters used in this study. The stability and preservation of the filter samples were therefore examined via ion charge balance. The charge equivalence ratio of the sum of anions to cations exhibited a strong linear correlation for all samples (R $^2=0.98;\,p<0.01)$  with a slope of  $1.13\pm0.006$  (Fig. 2). This result is likely indicative that the PM $_{10}$  compositions have been well-preserved. We note that it is challenging to compare and contrast results from this study to results from networks such as the CSN because of the difference in collection techniques. Here we are focused on comparing the relative changes over time in two different environments (urban vs. rural) that utilized the same sampling protocols such that the records are directly comparable.

The time series of inorganic chemical compositions of  $PM_{10}$  observed in urban and rural areas in RI from 2005 to 2015 are presented in Fig. 3. For the entire measurement period,  $pSO_4$  and pNa were the most abundant components of  $PM_{10}$  in both urban and rural areas in terms of

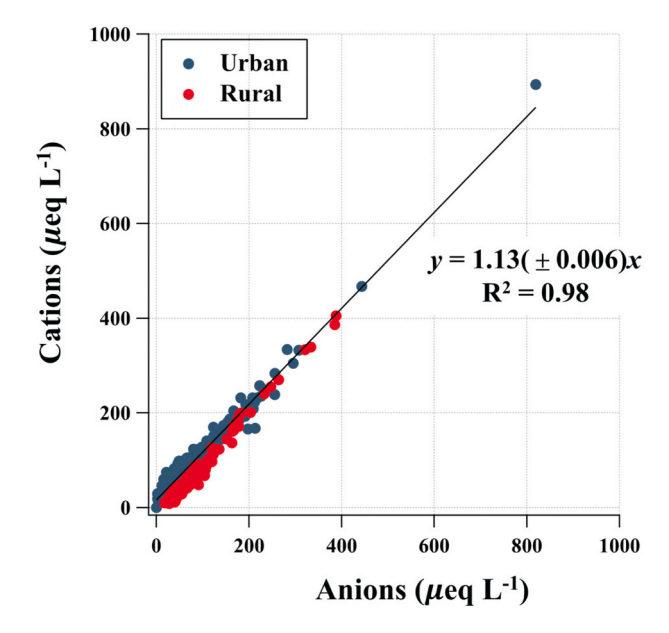


**Fig. 2.** Total cations versus total anions equivalence for all of the  $PM_{10}$  samples (n=873) in Rhode Island from 2005 to 2015.

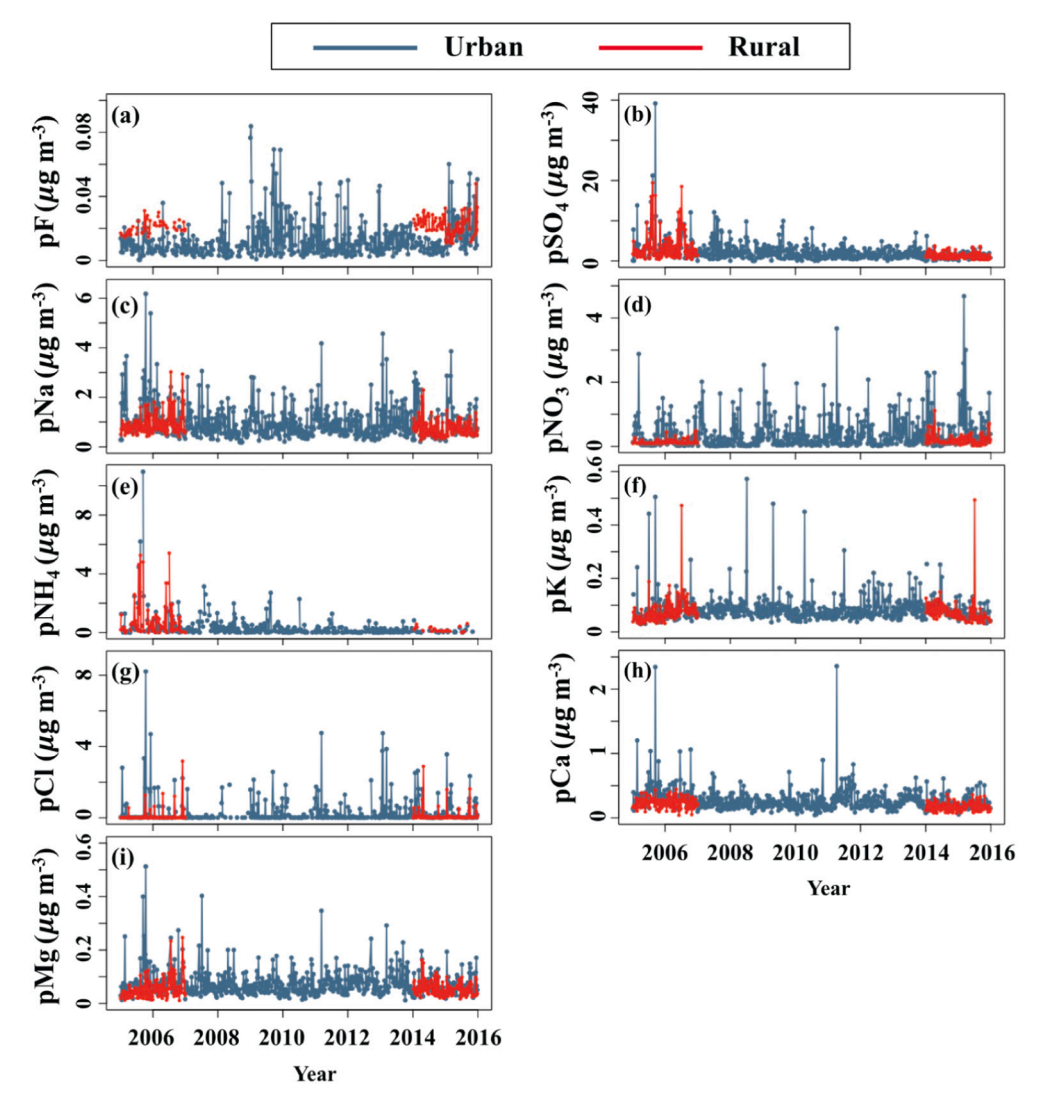


Fig. 3. Time series of the concentrations of inorganic components (e.g., pF, pSO<sub>4</sub>, pNa, pNO<sub>3</sub>, pNH<sub>4</sub>, pK, pCl, pCa, and pMg) of PM<sub>10</sub> observed in RI from 2005 to 2015.

mass fraction (Fig. S1). The pSO<sub>4</sub> and pNa account for 47 % and 21 % in the urban site and 52 % and 18 % in the rural site of the total inorganic compositions, with median values of 1.6  $\mu g~m^{-3}$  and 0.8  $\mu g~m^{-3}$  for urban and 1.5  $\mu g~m^{-3}$  and 0.7  $\mu g~m^{-3}$  for rural, respectively. On the other hand, in terms of mole fraction, pNa was the most abundant species in the urban (37 %), followed by pSO<sub>4</sub> (20 %) and pNH<sub>4</sub> (18 %), while pNH<sub>4</sub> (36 %) was the highest in the rural area followed by pNa (29 %) and pSO<sub>4</sub> (21 %).

Short-term events with elevated inorganic concentrations characterized both the urban and rural records. High concentrations of pSO<sub>4</sub> were frequently observed in conjunction with elevated pNH<sub>4</sub> concentrations at the urban site, especially in the early years of the aerosol record (Fig. 3b, e). For example, the maximum pSO<sub>4</sub> and pNH<sub>4</sub> concentrations reached 39.2  $\mu$ g m<sup>-3</sup> and 11.0  $\mu$ g m<sup>-3</sup> in September 2005. In the urban area, a strong correlation between pSO<sub>4</sub> and pNH<sub>4</sub> exists for the entire period ( $R^2 = 0.93$ ). Similarly, pNa and pCl are also well correlated ( $R^2 = 0.77$ ), with a local maximum in concentrations of both species occurring in October 2005 at the urban site. Significant correlations were also observed between pSO<sub>4</sub> and pCa ( $R^2 = 0.60$ ), pNa and pMg ( $R^2 = 0.58$ ), and pNa and pNO<sub>3</sub> ( $R^2 = 0.57$ ). In the rural area, a strong correlation was found between pSO<sub>4</sub> and pNH<sub>4</sub> ( $R^2 = 0.97$ ), but their high concentration events did not overlap with the timing of those in the urban area. Moreover, high pNa concentrations in the rural area

were observed with high pMg concentrations. Indeed, pNa had a stronger correlation with pMg ( $R^2=0.81$ ) than with pCl ( $R^2=0.58$ ). Significant correlations were also observed between pSO<sub>4</sub> and pCa ( $R^2=0.59$ ) and pMg and pCl ( $R^2=0.50$ ). The correlations for other species can be found in Fig. S2.

Significant spatial differences between the urban and rural sites were observed (Fig. 4). The spatial comparison was conducted for 2005, 2006, 2014, and 2015, which were available years for both sites. The total mass concentration of inorganic compositions in the urban area was usually higher than in the rural area (p < 0.05). In addition to total mass, there were differences in the inorganic components of PM<sub>10</sub> between the urban and rural sites. In the rural site, pF was significantly higher than in the urban site (p < 0.01; Table S1). The average pNH<sub>4</sub> concentrations were higher than in the urban area, but this was not found to be statistically significantly different (p = 0.25). On the other hand, significantly higher concentrations of pNO<sub>3</sub> (p < 0.01) and sea salt aerosol compositions such as pNa, pCl, pMg, and pCa (p < 0.01) were observed in the urban area relative to the rural area, as expected due to the location of the sites relative to the coastline (Fig. 1).

From 2005 to 2015, the total mass of inorganic chemical compositions of  $PM_{10}$  considerably decreased (Fig. 5a), though the percent change has dramatically slowed during the most recent 5 years (from 2011 to 2015). For the entire sampling period (2005 to 2015), the total

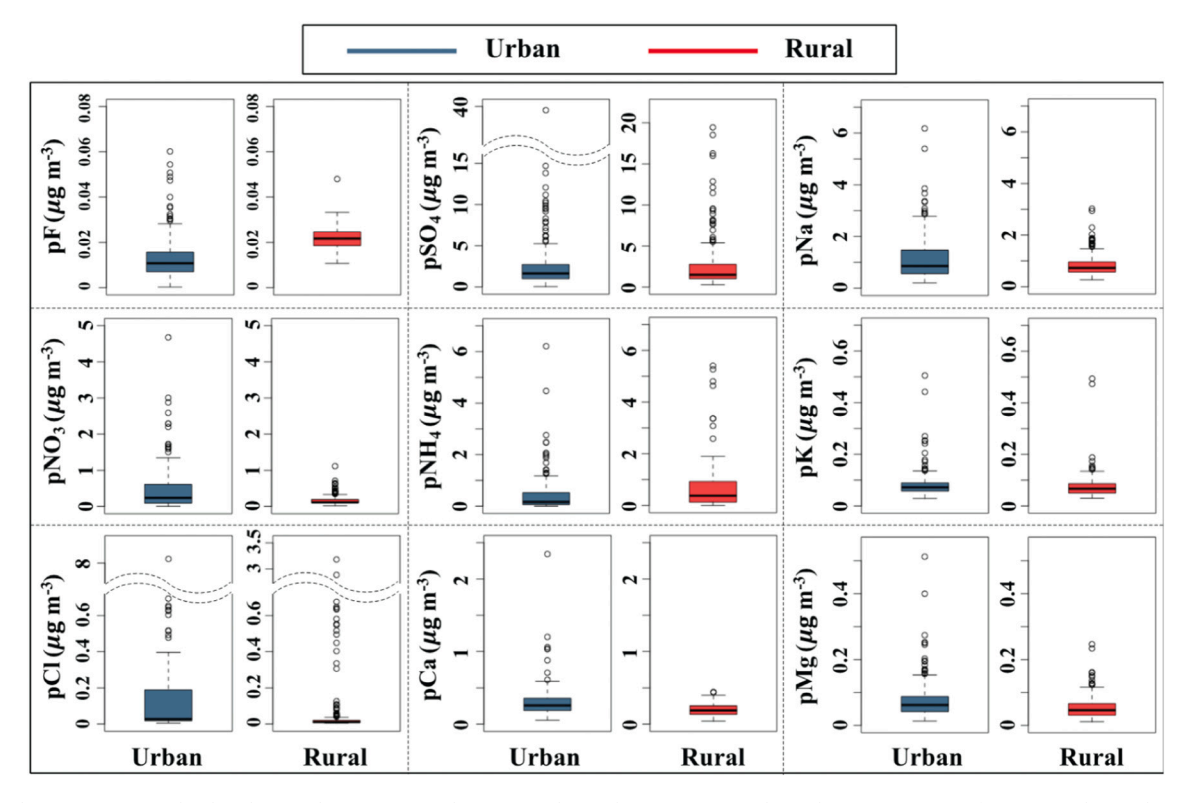


Fig. 4. Box plots summarizing the distribution (lower extreme, lower quartile, median, upper quartile, and upper extreme) of inorganic chemical compositions of  $PM_{10}$  for urban and rural areas. The plot is for 2005, 2006, 2014, and 2015, which were available years for both urban and rural sites.

mass of inorganic compositions decreased from 8.1 ( $\pm 8.4$ )  $\mu g \, m^{-3}$  to 3.8 ( $\pm 2.2$ )  $\mu g \, m^{-3}$  and from 5.3 ( $\pm 5.3$ )  $\mu g \, m^{-3}$  to 2.6 ( $\pm 1.1$ )  $\mu g \, m^{-3}$  for urban and rural areas, respectively. However, in the early years (2005 to 2010), the average rate of change downward in the total mass concentration of ions was  $-14~\%~yr^{-1}$ . In contrast, in the most recent years (2011–2015), the total mass concentration oscillates between increases and decreases, resulting in an overall change of only -2~% during this period.

Major components of inorganic contributions to PM<sub>10</sub> mass have also changed with time (Fig. 5a). In the early years, the major component comprising PM<sub>10</sub> was pSO<sub>4</sub>; however, pSO<sub>4</sub> mass has dramatically decreased in urban and rural areas in the more recent years of the aerosol record. Additionally, pNH4 showed elevated concentrations in the early years but was barely detected at the urban and rural sites in the most recent years (2011–2015). Overall, pNH<sub>4</sub> and pSO<sub>4</sub> concentrations in  $PM_{10}$  decreased by 88 % and 70 %, and 78 % and 65 % in urban and rural areas, respectively. In contrast to the decreasing trend in pSO<sub>4</sub> and pNH<sub>4</sub> concentrations, pNO<sub>3</sub> concentrations have increased by 90 % and 57 % for urban and rural areas, respectively. The primary sea-salt and crustal inorganic PM<sub>10</sub> components, including pNa, pK, pMg, pCa, and pCl indicated a consistent mass contribution throughout the record. As a result, the relative contributions of various inorganic components to PM<sub>10</sub> have changed over time. At the beginning of the aerosol record, pSO<sub>4</sub> accounted for nearly two-thirds of the total PM<sub>10</sub> mass, but the proportion decreased to 30 % in recent years. In concert, the relative proportions of pNa, pCl, pCa, and pNO<sub>3</sub> increased up to 60 % in the urban and rural areas.

The seasonality of major inorganic and anthropogenic components of pNO<sub>3</sub>, pSO<sub>4</sub>, and pNH<sub>4</sub> have changed over time from 2005 (red) to 2015 (blue) (Fig. 6). For pNO<sub>3</sub>, concentrations were higher in the cold season (from Oct to Mar) than in the warm season (from Apr to Sep), and this seasonality has become more prominent in recent years. We note that recent spatiotemporal variations of pNO<sub>3</sub> concentrations in the northeastern US region are similar (Bekker et al., 2023; Kim et al., 2023). Contrary to pNO<sub>3</sub>, the monthly average pSO<sub>4</sub> and pNH<sub>4</sub> concentrations

have well-correlated seasonal variations over time, which were high in the warm season and low in the cold season in the early years. Comparison of the annual seasonality of  $pSO_4$  and  $pNH_4$  demonstrated considerable variability from the early to late 2000s. The largest decrease in  $pSO_4$  and  $pNH_4$  concentrations occurred in the warm season, resulting in a lack of seasonality in the latest years of the record.

## 3.2. Source apportionment

The total marine, crustal, and anthropogenic contributions to the ionic components in PM<sub>10</sub> for the ten-year record were calculated for the urban and rural sites (Fig. 5b). Overall, the anthropogenic inorganic contribution was the dominant source accounting for 60 % and 66 % at the urban and rural sites, respectively, followed by sea salt (34 % for urban and 29 % for rural) and crustal (6 % for urban and 5 % rural) sources (Fig. S3). Between the beginning and ending years of the time series, total anthropogenic contribution prominently decreased from 67 % to 47 % and from 77 % to 49 % in the urban and rural sites, respectively (Fig. 5b). In particular, anthropogenic pSO<sub>4</sub> accounted for a large portion of total anthropogenic contributions at the beginning of the record but dramatically decreased from 4.1 to 1.0  $\mu$ g m<sup>-3</sup> and from 3.2 to 1.0  $\mu g \ m^{-3}$  for the urban and rural site, respectively. This change in mass corresponded to a decrease of 75 % and 70 % for the urban and rural sites, respectively. Due to the changes in anthropogenic contributions, the relative fraction of the crustal source to inorganic PM<sub>10</sub> increased by a factor of 1.9 for the urban and a factor of ~3 for the rural site, and the sea salt source increased by 1.6 times for the urban site and 2.1 times for the rural site. The relative contribution of sea salt and crustal sources increased despite their mass contributions remaining consistent throughout the record, which averaged 1.6  $\mu g \ m^{-3}$  and 1.2  $\mu g$  $m^{-3}$  for sea salt and 0.3  $\mu g \; m^{-3}$  and 0.2  $\mu g \; m^{-3}$  for crustal at the urban and rural sites, respectively.

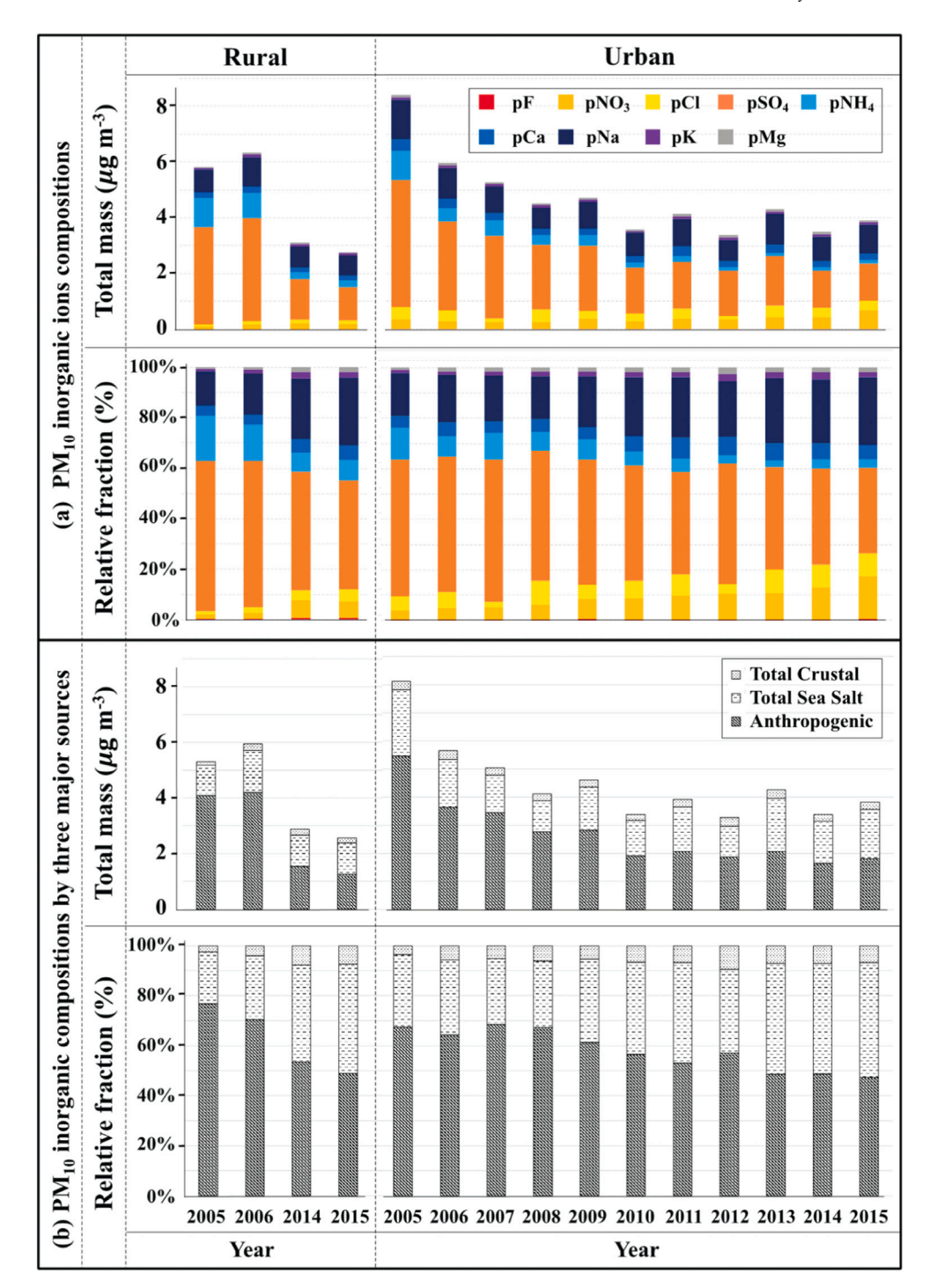


Fig. 5. Temporal variations of total mass concentration and relative fraction of (a)  $PM_{10}$  inorganic ion compositions and (b) the compositions by major sources such as crustal, sea salt, and anthropogenic from 2005 to 2015 for urban and rural areas.

# 3.3. Potential source contribution function (PSCF) analysis

PSCF analysis was applied to identify potential sources regions of the main anthropogenic components (i.e., pNO $_3$ , pSO $_4$ , and pNH $_4$ ) for the 2005–2006 (beginning), 2009–2010 (middle), and 2014–2015 (end) periods of the record for Providence and 2005–2006 (beginning) and 2014–2015 (end) for West Greenwich. The calculated PSCF values of pNO $_3$ , pSO $_4$ , and pNH $_4$  from 2005 to 2015 are shown in Fig. 7. The color in the maps corresponds to a probability, indicating the likelihood of a source region for a given species measured at the receptor site. The PSCF results identified the northeastern US (e.g., Connecticut, New Jersey,

New York, Pennsylvania, Massachusetts, New Hampshire, Rhode Island, and Vermont) as the main sources region contributing to pNO $_3$ , pSO $_4$ , and pNH $_4$  in PM $_{10}$  in RI. No major differences in spatial distributions of the calculated PSCF values were found between urban and rural areas (see PSCF results for West Greenwich in Fig. S4). Generally, PSCF results between pNO $_3$  and pSO $_4$  showed similar patterns in RI, but pNH $_4$  showed different tendencies. The main potential source areas of pNO $_3$  and pSO $_4$  were consistent between 2005 and 2015, with an average area of 458,000 km $^2$  and extending as much as 3000 km from the receptor site. However, the potential source area for pNH $_4$  gradually diminished from 2005 to 2015, with a source contribution area of 280,150 km $^2$  to

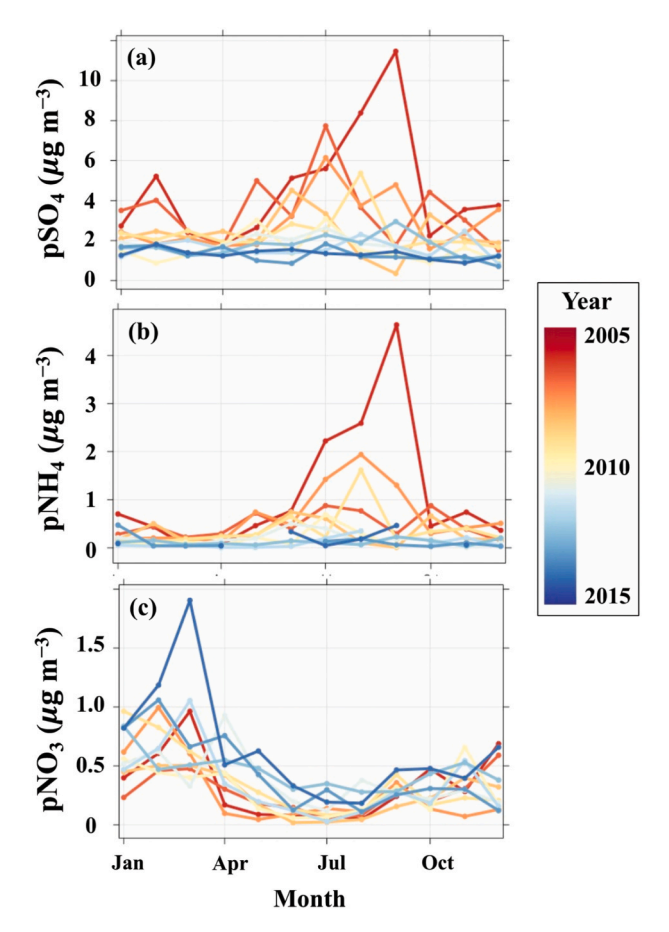


Fig. 6. Seasonal variations of (a)  $pSO_4$ , (b)  $pNH_4$ , and (c)  $pNO_3$  in  $PM_{10}$  from 2005 (red) to 2015 (blue).

 $22,850 \text{ km}^2$ . Furthermore, the greatest transport distance from 2005 to 2006 to 2014–2015 diminished from 3300 km to 1300 km, respectively. Thus, the potential sources contributing to pNH<sub>4</sub> for 2014–2015 were

more localized than in previous years. Overall, no significant transport or source-contributing region changes were identified for pNO<sub>3</sub> or pSO<sub>4</sub>.

The annual trends of the major inorganic  $PM_{10}$  anthropogenic precursor emissions, including  $NO_x$ ,  $SO_2$ , and  $NH_3$ , from 2005 to 2015 for the contiguous US and the northeastern US (e.g., Connecticut, New Jersey, New York, Pennsylvania, Massachusetts, New Hampshire, Rhode Island, and Vermont) are shown in Fig. 8. Considerable reductions of national  $NO_x$  and  $SO_2$  emissions have been observed throughout the US, with a total decrease of 43 % and 73 % between 2005 and 2015. Both  $NO_x$  and  $SO_2$  emissions in the northeastern US followed the reductions by 82 % and 46 %, respectively. On the other hand,  $NH_3$  emissions have shown little change in the US.  $NH_3$  emissions remained relatively consistent across the US, with slight increases until 2010 and then a slight decrease until 2015. Contrary to the nationwide trend,  $NH_3$  emissions have decreased in the northeastern US, though the relative reduction (35 %) was much lower than the  $NO_x$  and  $SO_2$  reductions.

#### 4. Discussion

#### 4.1. Natural sources of inorganic PM<sub>10</sub>

Over the past decade, the total mass concentration of  $PM_{10}$  from natural sources in RI has shown no significant variability, indicating a consistent contribution of crustal and sea salt sources (e.g., pCl, pSO<sub>4</sub>, and non-volatile cations (NVCs)). However, their relative contribution to the inorganic aerosol compositions has increased due to the decrease in anthropogenic contribution in recent years. The relative importance of sea salt has gradually increased and accounted for nearly 45 % of the total mass of inorganic  $PM_{10}$  in recent years for both urban and rural sites. Moreover, sea salt aerosol compositions such as pNa, pCl, and pMg were strongly correlated in this region, suggesting that the study area is heavily influenced by the nearby marine environment (Fig. S2).

Sodium chloride (NaCl), magnesium chloride (MgCl<sub>2</sub>), and calcium chloride (CaCl<sub>2</sub>) are all major components of sea salt particles. In particular, NaCl is the most abundant component in sea salt aerosols contributing to >80% of the mass. Interestingly, our record shows that pCl/pNa ratios in the study region (0.19 for the urban and 0.08 for the rural) were significantly lower than typical seawater (1.81; McInnes

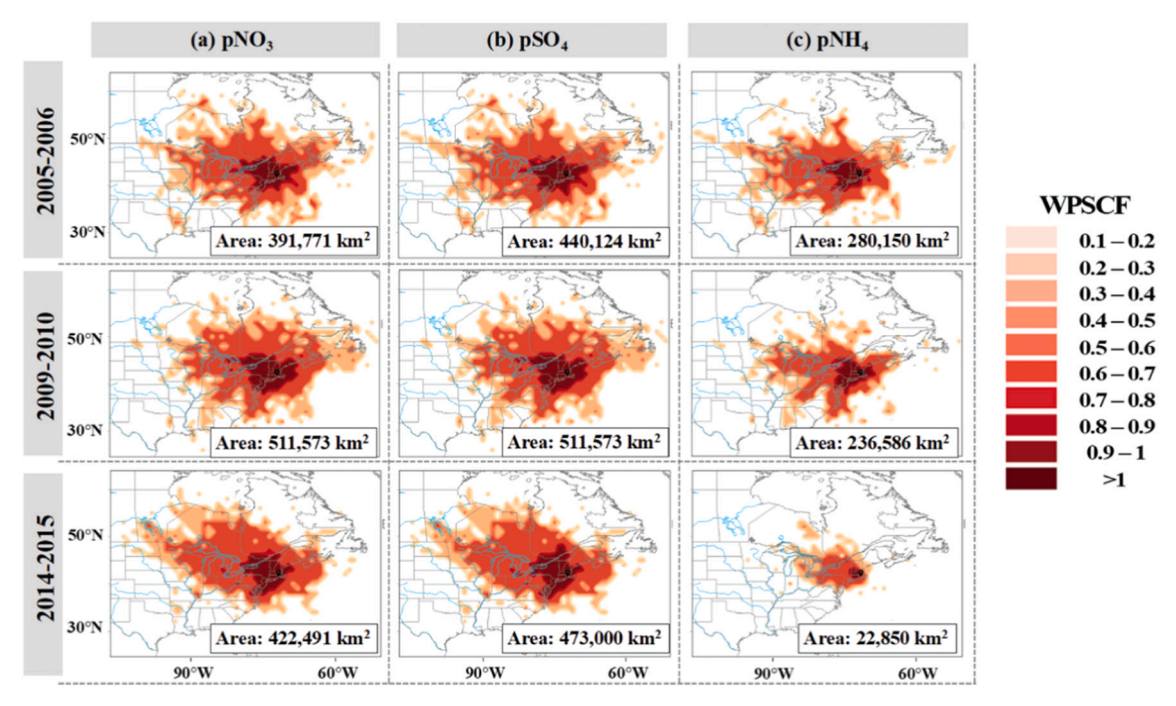


Fig. 7. Annual mean WPSCF maps for (a) pNO<sub>3</sub>, (b) pSO<sub>4</sub>, and (c) pNH<sub>4</sub> for 2005-2006 (beginning), 2009-2010 (middle), and 2014-2015 (end).

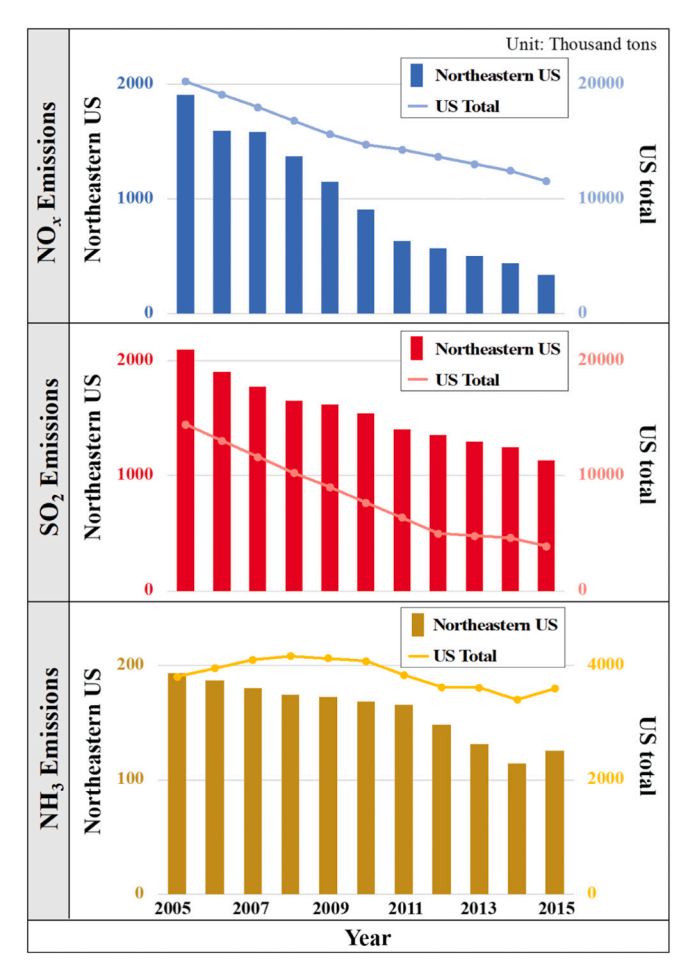


Fig. 8. Temporal variations for  $NO_x$ ,  $SO_2$ , and  $NH_3$  emissions in the northeastern US and total US from 2005 to 2015.

et al., 1994), suggesting an "aged" sea salt with a dominance of pCl depletion. The estimated pCl depletion (Eq. (15)) was approximately 89 % for the urban and 95 % for the rural area, with seasonal variation ranging from 86 % in the cold season to up to 98 % in the warm season. This depletion was larger than that reported in previous studies. For example, Zhao and Gao (2008) reported that pCl depletion varied from 14 % to 96 % depending on the particle size in Newark, New Jersey, US. In Italy, Cesari et al. (2018) also reported that pCl was depleted by about 60 %, suggesting the presence of aged sea spray at an urban background site.

%Chloride Depletion = 
$$(1.81 \times pNa - pCl)/(1.81 \times pNa) \times 100\%$$
 (15)

The pCl in sea salt particles can undergo acid displacement leading to the formation of gas-phase hydrochloric acid (HCl). At the same time, NVCs in sea salt interact with sulfuric acid ( $H_2SO_4$ ) and nitric acid ( $HNO_3$ ) by strongly modulating the aerosol acidity ( $Guo\ et\ al.,\ 2018$ ), resulting in fine and coarse aerosol formation, including sodium sulfate ( $Na_2SO_4$ ; (R1)), sodium nitrate ( $NaNO_3$ ; (R2)), and calcium sulfate ( $CaSO_4$ ):

$$2NaCl(s) + H_2SO_4(g) \rightarrow 2HCl(g) + Na_2SO_4(s)$$
 (R1)

$$NaCl(s) + HNO_3(g) \rightarrow HCl(g) + NaNO_3(s)$$
 (R2)

A stronger correlation between pNa and pNO $_3$  ( $R^2=0.57$  at the urban and 0.43 at the rural site) was observed compared to the correlation between pNa and pSO $_4$  ( $R^2=0.33$  for the urban and 0.36 for the rural). These observations suggest that pCl was primarily displaced in the form of NaNO $_3$  by the reaction between HNO $_3$  and sea salt than

Na<sub>2</sub>SO<sub>4</sub> in this region. HCl, which is produced by pCl depletion has higher volatility relative to HNO3, resulting in little impact on the pH (Guo et al., 2018). Further, our record also indicated that pSO<sub>4</sub> was well correlated with pCa ( $R^2 = 0.60$  for the urban and 0.59 for the rural). These correlations suggest that the NVCs, particularly pNa and pCa, play an important role in neutralizing H<sub>2</sub>SO<sub>4</sub> and HNO<sub>3</sub> in addition to pNH<sub>4</sub> during this period. Moreover, in recent years (e.g., 2014–2015), the correlation coefficient between pNa and pNO<sub>3</sub> reached up to 0.80 in the urban area (Fig. S6). Due to the massive reduction in atmospheric acid precursors, chloride depletion diminished from 2005 to 2015; though, it was still important for pNO3 incorporation into aerosol. This might be related to the fact that a decrease in H<sub>2</sub>SO<sub>4</sub> concentration from the SO<sub>2</sub> emissions reduction allows more NVCs to react with HNO<sub>3</sub> compared to the previous years. Therefore, our results highlight that the relative role of NaNO<sub>3</sub> is more important to aerosol formation than in previous years, which contributes to the increase in local pNO<sub>3</sub> concentration together with ammonium nitrate (NH4NO3) in recent years. Overall, the increasing contribution of sea salt in our sites underscores the importance of pCl depletion and NVCs in controlling aerosol formation in our study area.

# 4.2. Anthropogenic changes of major inorganic species in PM<sub>10</sub>

#### 4.2.1. Potential source region changes between 2005 and 2015

The northeastern US and its surroundings have been identified as the main potential source region of anthropogenic pSO<sub>4</sub> and pNO<sub>3</sub>, which has remained quite consistent over the 10 years (Fig. 7). According to the US Energy Information Administration, SO<sub>2</sub> and NO<sub>x</sub> emissions from electricity generation, coal-fired power plants, domestic combustion, and manufacturing processes have been considerably cut since 1990 under the CAAA in the US (US EPA, 2017; US EIA, 2018). However, the NEI estimates that the relative SO<sub>2</sub> fossil-fuel combustion emissions in New England have shifted from coal-dominated (52.6 % in 2008) to oildominated (81.6 % in 2014) in recent years (NEI, 2017), with oil burning still contributing importantly to NO<sub>x</sub> emissions. Additionally, the transportation sector still accounts for more than half of the total  $NO_x$  emissions in this region (NEI, 2017). Thus, even though precursor emissions have dramatically decreased in this region, the relative contribution to near-surface pSO<sub>4</sub> or pNO<sub>3</sub> concentration could vary depending on the emission sources over time. Note that PSCF is determined by the relative importance of the emissions from the source areas to the receptor sites, rather than the absolute amount of emissions. Therefore, given that the PSCF results consistently point to the northeastern US and its surroundings as the major sources region of pSO<sub>4</sub> and pNO<sub>3</sub> over the years, regional influences via long-range transport continue to be important in determining PM<sub>10</sub> composition. However, our results also indicate clear changes in chemical influences on PM<sub>10</sub> composition.

In contrast to pNO<sub>3</sub> and pSO<sub>4</sub>, pNH<sub>4</sub> shows a significant change in the source region contribution based on the PSCF analysis. While the potential source region for pNH<sub>4</sub> was similar to pNO<sub>3</sub> and pSO<sub>4</sub> in the early years, it has become much more localized in recent years. Gaseous NH3 plays an important role in neutralizing acid gases in the atmosphere and is converted into pNH4 through gas-to-particle conversion (Seinfeld and Pandis, 2016). Accordingly, the lifetime of total ammonium, NH<sub>x</sub> (NH<sub>3</sub> + pNH<sub>4</sub>), can be determined by the reactions with acid gases, leading to the formation of pSO<sub>4</sub> and pNO<sub>3</sub> in the atmosphere. The localized trend of pNH<sub>4</sub> from PSCF in recent years implies that the lifetime of NH<sub>x</sub> has decreased substantially across the years due to the reduction of pSO<sub>4</sub>. Reduced SO<sub>2</sub> emissions changed the aerosol pH, affecting the equilibrated partitioning of semivolatile compounds, such as NH<sub>4</sub>NO<sub>3</sub>, which has increased in recent years. Due to the semivolatile characteristics of NH<sub>4</sub>NO<sub>3</sub>, the gas-to-particle partitioning of NH<sub>x</sub> favors NH<sub>3</sub> remaining in the gas phase at the higher pH of recent years, consequently leading to a more localized source contribution to pNH<sub>4</sub>.

Agriculture activities such as livestock waste management and

fertilizer production are known to be dominant NH<sub>3</sub> emission sources in the US (NEI, 2017). However, in urban areas, NH3 from vehicles and fuel-combustion emissions have been identified as important sources (Decina et al., 2017; Walters et al., 2020, 2022). As the NH<sub>x</sub> lifetime changes with SO<sub>2</sub> emission change, the main source of gas-phase NH<sub>3</sub> for pNH<sub>4</sub> formation has also changed. In the early years of the observations, elevated PSCF probabilities for pNH4 indicated that potentially significant pNH<sub>4</sub> source regions originated from the northeastern US, including the midwestern US and southeastern Canada, which have significant agricultural-related NH3 emissions. Thus, long-range transport from the agriculture sector was likely the primary source of NH3 to our measurement site in the early years. On the other hand, localized PSCF probabilities in recent years imply that potential sources of pNH<sub>4</sub> have been confined within the northeastern US. This indicates that as NH<sub>x</sub> long-range transport decreased, local NH<sub>x</sub> emissions, such as vehicles and fuel-combustion emissions, have become increasingly important in our study sites. This is consistent with recent isotopic investigations conducted in RI, which show an important role for nonagriculture sources such as mobile and fuel-combustion emissions contributing to pNH<sub>4</sub> in the northeastern US (Walters et al., 2020, 2022).

#### 4.2.2. Spatial differences in anthropogenic inorganic species

As a result of  $SO_2$  emissions reduction in the US, the mass fraction of pSO<sub>4</sub> from anthropogenic sources has decreased from 2005 to 2015, implying the effectiveness of emission regulations in combating anthropogenic pSO<sub>4</sub> pollution. pSO<sub>4</sub> had no spatial difference between the urban and the rural sites (p > 0.05), suggesting similar background levels across the sites over the ten-year aerosol record. pNH<sub>4</sub> concentrations significantly decreased by nearly 96 % at both sites (Fig. 5a), which was considerably higher than the reduction in NH<sub>3</sub> emissions in the northeastern US (34.8 %). While the spatial differences of pNH<sub>4</sub> were insignificant between the urban and rural areas in the early years (p = 0.35), significant spatial differences were observed for pNH<sub>4</sub> in recent years (p < 0.05).

Throughout the record, significant spatial differences were observed for pNO $_3$  despite the close location of the two sites (p < 0.01). Higher pNO $_3$  concentration was always observed in the urban site than in the rural site, which indicates that local NO $_x$  emissions are important sources of particulate pNO $_3$  concentrations in the urban area. On the other hand, low NO $_x$  concentrations in the rural area well represent the rural background of pNO $_3$ . Surprisingly, the pNO $_3$  concentration trend did not follow the large NO $_x$  emissions reduction, as pNO $_3$  increased over the ten-year aerosol record. Overall, the changes in pSO $_4$ , pNH $_4$ , and pNO $_3$  that did not always follow the change in precursor emissions highlight the importance of the non-linear chemistry associated with their formation. This chemistry is important to understand to make recommendations for decreasing the concentrations of these significant anthropogenic components of PM.

## 4.2.3. Changes in seasonality

The influences of emission regulations on major anthropogenic inorganic species (e.g., pNO<sub>3</sub>, pSO<sub>4</sub>, and pNH<sub>4</sub>) were well reflected in seasonality changes of the aerosol record. For example, while summertime pSO<sub>4</sub> peaks were mainly observed in the early years (e.g., 2005–2007), no significant seasonality was observed in recent years (e.g., 2013–2015). In the polluted mid-latitudes, SO<sub>2</sub> is oxidized to pSO<sub>4</sub> not only through gaseous hydroxyl radical (OH) but also through aqueous S(IV) oxidation in clouds involving hydrogen peroxide (H<sub>2</sub>O<sub>2</sub>), ozone (O<sub>3</sub>), or oxygen (O<sub>2</sub>), with a dependence on aerosol acidity ((R3)–(R6); Alexander et al., 2009; Stockwell and Calvert, 1983; Harris et al., 2013).

$$SO_2 + 2OH \rightarrow H_2SO_4 (g)$$
 (R3)

$$SO_2 + O_2 + H_2O \rightarrow H_2SO_4$$
 (aq) (R4)

$$SO_2 + H_2O_2 \rightarrow H_2SO_4 \text{ (aq)}$$
 (R5)

$$H_2SO_4 \rightarrow SO_4^{2-} + 2H^+$$
 (R6)

In the eastern US, model simulations suggest that S(IV) oxidation via H<sub>2</sub>O<sub>2</sub> in cloud water contributes to 46 % of pSO<sub>4</sub> formation, and gas phase reaction with OH is 35 % (Shah et al., 2018). Our observations of summertime pSO<sub>4</sub> peaks in the early aerosol record (e.g., 2005–2007) imply that the oxidants were sufficiently available to fully oxidize SO<sub>2</sub> to pSO<sub>4</sub> due to the photochemical production of oxidants relevant to SO<sub>2</sub> oxidation. On the other hand, SO2 oxidation in winter early in the aerosol record was likely limited by oxidant availability, specifically in cloud water, due to reduced sunlight and high SO2 concentrations relative to oxidant availability. Compared to summertime, we observed small wintertime pSO<sub>4</sub> peaks in the early years of the aerosol record that might be related to high SO<sub>2</sub> emissions due to increased seasonal heating demands. Compared to the early years of the aerosol record, pSO<sub>4</sub> peaks have been considerably flattened in recent years (e.g., 2013-2015) in both winter and summer. Wintertime SO2 oxidation has become less limited by the availability of oxidants due to the reduction of SO<sub>2</sub> emissions, such that a greater proportion of SO2 emissions have been oxidized during winter in recent years. This change in oxidation chemistry explains the relative change in pSO<sub>4</sub> concentrations that decreased less during winter (61 %) compared to summer (76 %) for

The seasonality of pNH<sub>4</sub> closely followed pSO<sub>4</sub> and exhibited a dramatic change despite a limited change in precursor NH<sub>3</sub> emissions (Figs. 6, 8). NH<sub>3</sub> plays an important role in controlling aerosol acidity by neutralizing  $\rm H_2SO_4$ ,  $\rm HNO_3$ , and  $\rm HCl$  (Seinfeld and Pandis, 2016). When NH<sub>3</sub> is sufficiently available, NH<sub>3</sub> preferentially neutralizes  $\rm H_2SO_4$  to form ammonium bisulfate (NH<sub>4</sub>HSO<sub>4</sub>) and ammonium sulfate ((NH<sub>4</sub>)<sub>2</sub>SO<sub>4</sub>) due to the low saturation vapor pressure of  $\rm H_2SO_4$  by the reaction (R7) (Seinfeld and Pandis, 2016). The excess NH<sub>3</sub> then reacts with HNO<sub>3</sub> to form NH<sub>4</sub>NO<sub>3</sub> through reaction (R8). Therefore, the pSO<sub>4</sub> and pNO<sub>3</sub> formation is sensitive to NH<sub>3</sub> concentration, temperature, and relative humidity (RH).

$$H_2SO_4(g) + 2NH_3(g) \rightarrow (NH_4)_2SO_4(s)$$
 (R7)

$$HNO_3(g) + NH_3(g) \rightarrow NH_4NO_3(s)$$
 (R8)

Given the observed strong correlation between pSO<sub>4</sub> and pNH<sub>4</sub> ( $R^2$  = 0.96), high pNH<sub>4</sub> concentration in the summer in the early years is associated with enhanced NH<sub>4</sub>HSO<sub>4</sub> and (NH<sub>4</sub>)<sub>2</sub>SO<sub>4</sub> formation. In the early years, anthropogenic inorganic PM10 was dominated by NH4HSO4 and (NH<sub>4</sub>)<sub>2</sub>SO<sub>4</sub>, leading to high aerosol acidity (low pH). However, as SO2 emissions have decreased in recent years, the seasonality of pNH4 diminished. In more recent years, the reaction with HNO3 to form NH<sub>4</sub>NO<sub>3</sub> has become important for pNH<sub>4</sub> formation and, therefore, more important for fine mode PM, leading to an increase in particle pH for PM<sub>10</sub>. This is supported by the significantly increased correlation coefficient between  $pNO_3$  and  $pNH_4$  (from -0.24 to 0.56) from 2005 to 2015, especially in the urban area (Fig. S6). In the early years, when SO2 concentrations were high, pNH<sub>4</sub> concentrations and coarse mode acidity were dependent upon the availability of SO<sub>2</sub> in this region. Whereas in the recent years of the aerosol record, NH3 has been a more important factor in controlling fine pNO<sub>3</sub> concentration by the reaction with HNO<sub>3</sub>

Compared to pSO<sub>4</sub> and pNH<sub>4</sub>, the pNO<sub>3</sub> seasonality has become more pronounced in recent years. In general, pNO<sub>3</sub> was characterized by higher concentration in the cold season than in the warm season. The gas-to-particle partitioning rate of  $HNO_3/pNO_3$  is mainly governed by temperature, RH, and aerosol pH (R9). The partitioning to pNO<sub>3</sub> is favorably shifted toward the particle phase at colder temperatures, higher RH, and higher particle pH (Seinfeld and Pandis, 2016). During the early years of the aerosol record, high pSO<sub>4</sub> content led to acidic aerosol pH, causing  $HNO_3/pNO_3$  partitioning to favor the gaseous

phase, leading to low pNO3 concentration.

$$HNO_3(g) \leftrightarrow H^+ + NO_3^-$$
 (R9)

In the more recent years of the aerosol record, pNO $_3$  concentrations have continuously increased, despite the reduction of NO $_x$  emissions. This non-linear response in pNO $_3$  concentration in the northeastern US might be related to changes in the relative contribution from local production, long-range transport, or chemical mechanisms associated with pNO $_3$  formation (Bekker et al., 2023; Kim et al., 2023). In terms of chemical influences, as pSO $_4$  concentration decreases, particle pH increases, creating more favorable conditions to shift from gaseous HNO $_3$  to pNO $_3$ , resulting in higher concentrations and significant seasonality of pNO $_3$  in the more recent years of the aerosol record.

In Guo et al., 2016 and Shah et al., 2018, the fraction of pNO<sub>3</sub> was simulated as a function of particle pH and temperature over the eastern US using a PM thermodynamic model. The pNO<sub>3</sub> fraction was sensitive to both aerosol pH and temperature change. In particular, the pNO<sub>3</sub> fraction exponentially increases under the same temperature as aerosol pH increases. In these model simulations, the pNO<sub>3</sub> fraction in an early year (e.g., 2007) was less significant than in a recent year (e.g., 2015) due to the low particle pH caused by high pSO<sub>4</sub> content. Further, the pNO<sub>3</sub> fraction was modeled to be insensitive to temperature in the early year, consistent with our record. However, the temperature sensitivity has gradually increased as pH increased due to the decrease in SO<sub>2</sub> emissions. Therefore, pNO3 formation has become more sensitive to temperature under changing atmospheric acidity due to emission regulations, leading to greater NH<sub>4</sub>NO<sub>3</sub> formation at colder temperatures. This change contributes to the more pronounced seasonality of pNO<sub>3</sub> in wintertime in more recent years of the aerosol record. Overall, pNO<sub>3</sub> formation is limited by the availability of NH3 and NVCs in the eastern US (Shah et al., 2018; Guo et al., 2018; Park et al., 2004), and further, chemical feedbacks driven by emission reductions impact pNO<sub>3</sub> enhancement as pSO<sub>4</sub> decreases.

# 5. Conclusion

We observed significant spatial-temporal variations of inorganic chemical species in PM<sub>10</sub> in urban and rural areas in southern New England from 2005 to 2015. Overall, we found that anthropogenic and natural sources influence aerosol formation in our study area. In response to emission regulation, the reduction of acid rain precursors (i. e., SO2 and NOx) and NH3 emissions have changed aerosol acidity over the years. Our records show that pSO<sub>4</sub> from anthropogenic sources has considerably decreased, implying the effectiveness of emission control on pSO<sub>4</sub> concentrations. Conversely, the reduction in SO<sub>2</sub> emissions promotes pNO<sub>3</sub> formation by releasing excess NH<sub>3</sub>, decreasing aerosol acidity. Despite the significant reduction in NO<sub>x</sub> emissions, pNO<sub>3</sub> has reversely responded with an increase of 76 % from 2005 to 2015. The lack of a pNO<sub>3</sub> decrease was driven by the chemical mechanism associated with pNO<sub>3</sub> partitioning. Our results indicated that the potential source regions contributing to pSO<sub>4</sub> and pNO<sub>3</sub> remain relatively unchanged over time, but better constraints are needed to pinpoint precursor emission source changes in these regions.

Compared to pSO<sub>4</sub> and pNO<sub>3</sub>, the fate of pNH<sub>4</sub> was more affected by interaction with other gases, aerosols, and fine particles. The reduction in SO<sub>2</sub> emissions has resulted in excess NH<sub>3</sub> being available to neutralize HNO<sub>3</sub>, leading to an increase in fine pNO<sub>3</sub> with a reduction in pNH<sub>4</sub>. Further, the relative importance of urban NH<sub>3</sub> emissions is gradually increasing in recent years, which might continuously affect the neutralizing and oxidizing capacity of the atmosphere as well as PM<sub>2.5</sub> and PM<sub>10</sub> concentrations in the future. Our observations support modeling studies that have suggested that pNO<sub>3</sub> would continue to increase since 2015, due to changes in atmospheric acidity (e.g., Shah et al., 2018). Additionally, regulating both local and transported sources of NH<sub>x</sub> emissions may represent a more effective way to mitigate air quality, considering pNO<sub>3</sub> formation is limited by the availability of NH<sub>3</sub>

in the northeastern US.

It is also critical to detail the role natural sources, such as sea salt and crustal material, plays as they significantly affect aerosol chemistry at our study sites. The pNa and pCl act as an indicator of sea salt influence, and low pCl/pNa ratios suggested that pCl depletion (about 79 % of Clat both sites) was dominant in the study region. Depleted pCl in sea salt aerosol allows more NVCs to react with H2SO4 and HNO3 with aerosol acidity neutralization, leading to a strong correlation between pNa and pNO<sub>3</sub>. Overall, natural sources (e.g., sea salt and crustal) play an important role, and their influence on local production of fine and coarse PM levels has increased as anthropogenic emissions have decreased. Our results provide crucial insights into the complex relationship between atmospheric aerosol chemistry and emissions reduction. Considering similarities seen in recent aerosol chemistry across the northeastern US region (Bekker et al., 2023; Kim et al., 2023), these findings are likely broadly applicable, especially in urban coastal regions where significant NO<sub>x</sub>, SO<sub>2</sub>, and NH<sub>3</sub> emissions are present such as in western Europe and eastern China.

# CRediT authorship contribution statement

HK, WWW, and MGH designed the varying aspects of the study. HK and WWW carried out the laboratory measurements, interpreted data, and conducted statistical analysis. LK conducted trajectory analysis. HK, WWW, and MGH prepared the article with contributions from all coauthors.

# Declaration of competing interest

The authors declare that they have no known competing financial interests or personal relationships that could have appeared to influence the work reported in this paper.

# Data availability

Data presented in this article are available on the Harvard Dataverse at https://doi.org/10.7910/DVN/YZ1AGB.

# Acknowledgments

We thank Ruby Ho for laboratory assistance. We are grateful to the Rhode Island Department of Environmental Management (RI-DEM) and the Rhode Island Department of Health (RI-DOH).

# Financial support

This work was supported by the National Science Foundation [AGS-2002750].

# Appendix A. Supplementary data

Supplementary data to this article can be found online at https://doi.org/10.1016/j.scitotenv.2023.166848.

## References

Alexander, B., Hastings, M.G., Allman, D.J., Dachs, J., Thornton, J.A., Kunasek, S.A., 2009. Quantifying atmospheric nitrate formation pathways based on a global model of the oxygen isotopic composition ( $\Delta^{17}$ O) of atmospheric nitrate. Atmos. Chem. Phys. 9, 5043–5056.

Andreae, M.O., Jones, C.D., Cox, P.M., 2005. Strong present-day aerosol cooling implies a hot future. Nature 435, 1187–1190.

Ashbaugh, L.L., Malm, W.C., Sadeh, W.Z., 1985. A residence time probability analysis of sulfur concentrations at Grand Canyon National Park. Atmos. Environ. (1967) 19, 1263–1270.

Bekker, C., Walters, W.W., Murray, L.T., Hastings, M.G., 2023. Nitrate chemistry in the northeast US-part 1: nitrogen isotope seasonality tracks nitrate formation chemistry. Atmos. Chem. Phys. 23, 4185–4201.

- Berico, M., Luciani, A., Formignani, M., 1997. Atmospheric aerosol in an urban area—measurements of TSP and  $PM_{10}$  standards and pulmonary deposition assessments. Atmos. Environ. 31, 3659–3665.
- Bobbink, R., Hornung, M., Roelofs, J.G., 1998. The effects of air-borne nitrogen pollutants on species diversity in natural and semi-natural European vegetation. J. Ecol. 86, 717–738.
- Camargo, J.A., Alonso, Á., 2006. Ecological and toxicological effects of inorganic nitrogen pollution in aquatic ecosystems: a global assessment. Environ. Int. 32, 831–849.
- Cesari, D., De Benedetto, G.E., Bonasoni, P., Busetto, M., Dinoi, A., Merico, E., Chirizzi, D., Cristofanelli, P., Donateo, A., Grasso, F.M., 2018. Seasonal variability of PM<sub>2.5</sub> and PM<sub>10</sub> composition and sources in an urban background site in Southern Italy. Sci. Total Environ. 612, 202–213.
- Decina, S.M., Templer, P.H., Hutyra, L.R., Gately, C.K., Rao, P., 2017. Variability, drivers, and effects of atmospheric nitrogen inputs across an urban area: emerging patterns among human activities, the atmosphere, and soils. Sci. Total Environ. 609, 1524–1534.
- Delmas, R., 1981. Contribution à l'étude des forêts équatoriales comme sources naturellesde dérivés soufrés atmosphériques. PhD Thesis. Université Paul Sabatier de Toulouse, Toulose, France.
- Dominici, F., Daniels, M., Zeger, S.L., Samet, J.M., 2002. Air pollution and mortality: estimating regional and national dose-response relationships. J. Am. Stat. Assoc. 97, 100–111.
- Donaldson, K., Ian Gilmour, M., MacNee, W., 2000. Asthma and  $PM_{10}$ . Respir. Res. 1, 12–15.
- Fuzzi, S., Baltensperger, U., Carslaw, K., Decesari, S., Denier van der Gon, H., Facchini, M.C., Fowler, D., Koren, I., Langford, B., Lohmann, U., 2015. Particulate matter, air quality and climate: lessons learned and future needs. Atmos. Chem. Phys. 15, 8217–8299.
- Guo, H., Sullivan, A.P., Campuzano-Jost, P., Schroder, J.C., Lopez-Hilfiker, F.D., Dibb, J. E., Jimenez, J.L., Thornton, J.A., Brown, S.S., Nenes, A., 2016. Fine particle pH and the partitioning of nitric acid during winter in the northeastern United States. J. Geophys. Res. Atmos. 121, 10–355.
- Guo, H., Nenes, A., Weber, R.J., 2018. The underappreciated role of nonvolatile cations in aerosol ammonium-sulfate molar ratios. Atmos. Chem. Phys. 18, 17307–17323
- Harris, E., Sinha, B., Van Pinxteren, D., Tilgner, A., Fomba, K.W., Schneider, J., Roth, A., Gnauk, T., Fahlbusch, B., Mertes, S., 2013. Enhanced role of transition metal ion catalysis during in-cloud oxidation of SO<sub>2</sub>. Science 340, 727–730.
- Harrison, R.M., Deacon, A.R., Jones, M.R., Appleby, R.S., 1997. Sources and processes affecting concentrations of  $PM_{10}$  and  $PM_{2.5}$  particulate matter in Birmingham (UK). Atmos. Environ. 31, 4103–4117.
- Holt, J., Selin, N.E., Solomon, S., 2015. Changes in inorganic fine particulate matter sensitivities to precursors due to large-scale US emissions reductions. Environ. Sci. Technol. 49, 4834–4841.
- Huang, K., Zhuang, G., Xu, C., Wang, Y., Tang, A., 2008. The chemistry of the severe acidic precipitation in Shanghai, China. Atmos. Res. 89, 149–160.
- Hyslop, N.P., 2009. Impaired visibility: the air pollution people see. Atmos. Environ. 43, 182–195.
- Jaeglé, L., Shah, V., Thornton, J.A., Lopez-Hilfiker, F.D., Lee, B.H., McDuffie, E.E., Fibiger, D., Brown, S.S., Veres, P., Sparks, T.L., 2018. Nitrogen oxides emissions, chemistry, deposition, and export over the Northeast United States during the WINTER aircraft campaign. J. Geophys. Res. Atmos. 123, 12–368.
- Jayarathne, T., Stockwell, C.E., Yokelson, R.J., Nakao, S., Stone, E.A., 2014. Emissions of fine particle fluoride from biomass burning. Environ. Sci. Technol. 48, 12636–12644.
- Kennish, M.J., 2019. Practical Handbook of Marine Science. CRC press.
- Kim, H., Walters, W.W., Bekker, C., Murray, L.T., Hastings, M.G., 2023. Nitrate chemistry in the northeast US-part 2: oxygen isotopes reveal differences in particulate and gasphase formation. Atmos. Chem. Phys. 23, 4203–4219.
- Lenschow, P., Abraham, H.-J., Kutzner, K., Lutz, M., Preuß, J.-D., Reichenbächer, W., 2001. Some ideas about the sources of  $PM_{10}$ . Atmos. Environ. 35, S23–S33.
- Manisalidis, I., Stavropoulou, E., Stavropoulos, A., Bezirtzoglou, E., 2020. Environmental and health impacts of air pollution: a review. Front. Public Health 14.
- McInnes, L.M., Covert, D.S., Quinn, P.K., Germani, M.S., 1994. Measurements of chloride depletion and sulfur enrichment in individual sea-salt particles collected from the remote marine boundary layer. J. Geophys. Res. Atmos. 99, 8257–8268.
- Meng, Y., Zhao, Y., Li, R., Li, J., Cui, L., Kong, L., Fu, H., 2019. Characterization of inorganic ions in rainwater in the megacity of Shanghai: spatiotemporal variations and source apportionment. Atmos. Res. 222, 12–24.

- Nah, T., Yang, J., Wang, J., Sullivan, A.P., Weber, R.J., 2021. Fine aerosol acidity and water during summer in the eastern North Atlantic. Atmosphere 12, 1040.
- NEI (National Emissions Inventory), 2017. Retrieved From the United States Environmental Protection Agency. https://www.epa.gov/air-emissions-inventories/2017-national-emissions-inventory-nei-data last access: 24 April 2023.
- O'Dowd, C.D., Smith, M.H., Consterdine, I.E., Lowe, J.A., 1997. Marine aerosol, sea-salt, and the marine sulphur cycle: a short review. Atmos. Environ. 31, 73–80.
- Orellano, P., Reynoso, J., Quaranta, N., Bardach, A., Ciapponi, A., 2020. Short-term exposure to particulate matter (PM<sub>10</sub> and PM<sub>2.5</sub>), nitrogen dioxide (NO<sub>2</sub>), and ozone (O<sub>3</sub>) and all-cause and cause-specific mortality: systematic review and meta-analysis. Environ. Int. 142, 105876.
- Park, R.J., Jacob, D.J., Field, B.D., Yantosca, R.M., Chin, M., 2004. Natural and transboundary pollution influences on sulfate-nitrate-ammonium aerosols in the United States: implications for policy. J. Geophys. Res. Atmos. 109.
- Pye, H.O., Nenes, A., Alexander, B., Ault, A.P., Barth, M.C., Clegg, S.L., Collett Jr., J.L., Fahey, K.M., Hennigan, C.J., Herrmann, H., 2020. The acidity of atmospheric particles and clouds. Atmos. Chem. Phys. 20, 4809–4888.
- Scanlon, P.D., Connett, J.E., Waller, L.A., Altose, M.D., Bailey, W.C., Sonia Buist, A., Lung Health Study Research Group, D.P.T. for the, 2000. Smoking cessation and lung function in mild-to-moderate chronic obstructive pulmonary disease: the lung health study. Am. J. Respir. Crit. Care Med. 161, 381–390.
- Schlesinger, R.B., 2007. The health impact of common inorganic components of fine particulate matter (PM<sub>2.5</sub>) in ambient air: a critical review. Inhal. Toxicol. 19, 811–832.
- Seinfeld, J.H., 1998. Clouds, contrails and climate. Nature 391, 837-838.
- Seinfeld, J.H., Pandis, S.N., 2016. Atmospheric Chemistry and Physics: From Air Pollution to Climate Change. John Wiley & Sons.
- Shah, V., Jaeglé, L., Thornton, J.A., Lopez-Hilfiker, F.D., Lee, B.H., Schroder, J.C., Campuzano-Jost, P., Jimenez, J.L., Guo, H., Sullivan, A.P., 2018. Chemical feedbacks weaken the wintertime response of particulate sulfate and nitrate to emissions reductions over the eastern United States. Proc. Natl. Acad. Sci. 115, 8110–8115.
- Sickles II, J.E., Shadwick, D.S., 2015. Air quality and atmospheric deposition in the eastern US: 20 years of change. Atmos. Chem. Phys. 15, 173–197.
- Stein, A.F., Draxler, R.R., Rolph, G.D., Stunder, B.J., Cohen, M.D., Ngan, F., 2015. NOAA's HYSPLIT atmospheric transport and dispersion modeling system. Bull. Am. Meteorol. Soc. 96, 2059–2077.
- Stockwell, W.R., Calvert, J.G., 1983. The mechanism of the HO-SO<sub>2</sub> reaction. Atmos. Environ. (1967) 17, 2231–2235.
- Sun, Y., Zhuang, G., Tang, A., Wang, Y., An, Z., 2006. Chemical characteristics of PM<sub>2.5</sub> and PM<sub>10</sub> in haze-fog episodes in Beijing, Environ. Sci. Technol. 40, 3148–3155.
- US EIA (Energy Information Administration), 2018. Changes in coal sector led to less SO<sub>2</sub> and NO<sub>x</sub> emissions from electric power industry. https://www.eia.gov/todayinenergy/detail.php?id=37752 (last access: 24 April 2023).
- US EPA (Environmental Protection Agency), 2017. Our nation's air. https://gispub.epa.gov/air/trendsreport/2017.
- USEPA—Method IO-2.1, 1999. IO Compendium Method IO-2.1: Compendium of Methods for the Determination of Inorganic Compounds in Ambient Air: Sampling of Ambient Air for Total Suspended Particulate Matter (SPM) and PM<sub>10</sub> Using High Volume (HV) Sampler (EPA/625/R-96/010a).
- Van Breemen, N., Van Dijk, H.F.G., 1988. Ecosystem effects of atmospheric deposition of nitrogen in the Netherlands. Environ. Pollut. 54, 249–274.
- Walters, W.W., Song, L., Chai, J., Fang, Y., Colombi, N., Hastings, M.G., 2020. Characterizing the spatiotemporal nitrogen stable isotopic composition of ammonia in vehicle plumes. Atmos. Chem. Phys. 20, 11551–11567.
- Walters, W.W., Karod, M., Willcocks, E., Baek, B.H., Blum, D.E., Hastings, M.G., 2022.Quantifying the importance of vehicle ammonia emissions in an urban area of northeastern USA utilizing nitrogen isotopes. Atmos. Chem. Phys. 22, 13431–13448.
- Wang, Y.Q., Zhang, X.Y., Arimoto, R., 2006. The contribution from distant dust sources to the atmospheric particulate matter loadings at XiAn, China during spring. Sci. Total Environ. 368, 875–883.
- Wang, Y.Q., Zhang, X.Y., Draxler, R.R., 2009. TrajStat: GIS-based software that uses various trajectory statistical analysis methods to identify potential sources from long-term air pollution measurement data. Environ. Model. Software 24, 938–939.
- Wilson, W.E., Suh, H.H., 1997. Fine particles and coarse particles: concentration relationships relevant to epidemiologic studies. J. Air Waste Manage. Assoc. 47, 1238–1249.
- Zeng, Y., Hopke, P.K., 1989. A study of the sources of acid precipitation in Ontario, Canada. Atmos. Environ. (1967) 23, 1499–1509.
- Zhao, Y., Gao, Y., 2008. Acidic species and chloride depletion in coarse aerosol particles in the US east coast. Sci. Total Environ. 407, 541–547.